**Title: Persistent effects of dietary selection and inbreeding on microbiome composition and longevity in Drosophila**

♀Peyton K. Warren, ORCID 0009-0003-6100-1381

♀Garrison Miller,

♂Gaurav S. Kandlikar, ORCID 0000-0003-3043-6780

♀Enoch Ng'oma ORCID 0000-0002-6741-7922

♀Division of Biological Sciences, University of Missouri-Columbia, MO, USA

♂Department of Biological Sciences, Louisiana State University, LA

Peyton K. Warren and Garrison Miller contributed equally to this work.

*Correspondence: Enoch Ng'oma

ngomae@missouri.edu

**Abstract**

Background

Dietary environments can shape host-microbe co-evolution by imposing selection pressures that favor host and microbial genotypes with enhanced fitness under specific nutritional conditions. However, the long-term evolutionary dynamics of these interactions after selection pressures are relaxed remain poorly understood. Here, we investigated the microbiome of *Drosophila melanogaster* populations that underwent long-term experimental evolution under three temporally variable nutritional regimes (constant high sugar, progressively decreasing protein, and fluctuating protein), and compared them to unselected controls. Following inbreeding of evolved populations, we examined how persistent evolutionary effects interact with aging to shape host-microbe relationships and survival.

Results

All selected regimes exhibited reduced survival relative to controls, indicating lasting physiological costs associated with historical selection and inbreeding. Survival differed among regimes: the deteriorating-protein regime was closest to controls, the fluctuating-protein regime was intermediate, and the high-sugar regime showed the shortest lifespan. Survival effects were sex-specific: relative to control females, those from the fluctuating-protein regime exhibited reduced early-life survival, whereas females from the deteriorating-protein regime experienced greater late-life mortality. Microbiome composition varied with both selection regime and age. Although Firmicutes and Proteobacteria dominated across groups, selected lines showed increased Firmicutes and reduced Proteobacteria, especially early in life, suggesting early-life taxonomic restructuring. The decreasing-protein regime maintained more stable microbial diversity over time, whereas high-sugar and fluctuating-protein diets were associated with progressive microbiome instability with age. Core *Acetobacter* species (*A. aceti*, *A. oryzifermentans*) declined in abundance in selected flies, indicating persistent disruption of

microbiome integrity. A random forest model predicted fly age from microbiome composition with 78.8% accuracy, reinforcing links between microbial dynamics and host aging.

## Conclusion

Historical dietary selection and inbreeding can leave lasting signatures on survival and microbiome composition in *Drosophila*. Protein restriction promoted late-life longevity and microbial stability, whereas high-sugar and fluctuating diets were associated with early-life effects followed by later-life shifts in dominant taxa. Together, these findings illustrate how nutritional history and its microbial legacies influence lifespan and aging through persistent host-microbe interactions.

**Keywords:** experimental evolution, nutritional history, longevity, microbiome legacies, dietary stress, persistent effects.

## Introduction

Microorganisms are deeply integrated into host biology across taxonomic and functional scales, playing critical roles in organismal performance and fitness (Ley et al. 2008; Muegge et al. 2011; Gould et al. 2018). Rapidly changing environmental conditions increase the pressure for hosts to cope with novel conditions faster than their genomes can evolve. Microbial genomes, which evolve more rapidly than host genomes, represent an important source of ecological and functional flexibility, enabling hosts to respond to environmental stressors through shifts in symbiotic composition and activity. Microbiotas, as part of the functional hologenome, can mediate developmental timing, immune defense, energy allocation, and other traits central to host survival and reproduction [4, 5]. In many species, the microbiome is a key modulator of host fitness [6], development [7, 8], reproduction [9, 10], stress tolerance [11], pathogenic defense [12, 13], survival, and aging [13–15]. Disruptions to microbial composition can increase gut permeability and systemic inflammation, accelerating physiological decline [16], whereas beneficial microbes can attenuate immune overactivation and extend lifespan [14]. These findings position inflammation as a central axis through which microbiotas mediate life-history trade-offs, particularly under dietary stress [14, 16], reviewed in [17, 18].

Diet is a dominant ecological determinant of host-associated microbiomes. In *Drosophila melanogaster*, while variation in microbiome composition has been linked to host allele frequency shifts in genes associated with local adaptation [4], microbial composition is often more strongly influenced by the nutritional environment than host genotype [19, 20]. For example, *Lactobacillus plantarum* enhances larval growth on poor diets by promoting insulin signaling [7], while acetic acid bacteria regulate sugar metabolism and immune function [21]. Nutrient availability thus shapes both microbiota composition and downstream host traits including immune investment, somatic maintenance, and fecundity. Many studies have shown that reduced protein-to-carbohydrate (P:C) ratios extend lifespan at the cost of reproductive

output, whereas protein-rich diets promote early-life fecundity but reduce survival [22–24]. These physiological responses are mediated through nutrient-sensing pathways such as IIS and mTOR [25, 26], which are also modulated by gut microbes [27]. Given this complex interplay, sustained dietary stress is expected to shape host physiology and microbiome composition in concert.

Intrinsic host factors such as age also interact with microbial dynamics. In *D. melanogaster*, aging is associated with shifts in gut microbiota composition, including reduced diversity and expansion of inflammatory taxa [14, 28]. These changes are not simply passive consequences of aging but actively contribute to age-related physiological decline, suggesting that the microbiome is both a target and mediator of aging processes.

Here, we examine a set of experimentally evolved *D. melanogaster* populations that were maintained for 65 generations under distinct dietary selection regimes and subsequently inbred for >30 generations due to COVID pandemic-related disruptions. This design enables us to investigate whether long-term dietary selection has left lasting genomic or microbiome signatures that persist after extended inbreeding and rearing under a common diet. Selection treatments included: 1) deteriorating availability (DA), representing high-to-low protein provision within each generation; 2) fluctuating availability (FA), reflecting predictable high-low-high protein cycles; and 3) constant high sugar (CH), modeling persistent metabolic excess. A control group (C) was maintained without dietary stress.

Our primary goal was to determine whether historical dietary selection is reflected in contemporary microbiome composition and host survival patterns. We therefore refer to any observed differences as *legacies of dietary history* rather than direct evidence of ongoing adaptation. We hypothesized that hosts derived from contrasting nutritional histories would

118 retain distinct microbiome compositions reflecting their ancestral environments, potentially
119 influencing lifespan through pathways linked to inflammation and metabolic homeostasis.
120
121 Specifically, we predicted that the DA regime would show signatures consistent with investment
122 in somatic maintenance and longevity, potentially mediated by microbes that mitigate
123 inflammatory processes. In the FA regime, evolved under predictable cycles of abundance and
124 scarcity, we anticipated intermediate survival outcomes and dynamically shifting microbial
125 compositions reflecting metabolic flexibility. Chronic high-sugar exposure (CH regime) was
126 expected to produce signatures of metabolic stress and reduced microbial diversity. Finally, we
127 anticipated that age-related microbiota succession would interact with these dietary legacies,
128 producing distinct temporal patterns of microbial resilience or instability.
129
130 Collectively, these predictions provide a framework for testing how long-term nutritional history,
131 filtered through both host and microbial evolution, can leave enduring effects on host–
132 microbiome interactions and life-history dynamics, even after prolonged inbreeding and
133 common-garden rearing.
134
135 **Materials and methods**
136 Experimental evolution
137 As part of a larger study, we experimentally evolved a population of *D. melanogaster* under
138 several stressful nutritional conditions. We generated the initial population by mass-
139 intercrossing 835 recombinant inbred lines from the B population (pB) of the *Drosophila*
140 Synthetic Population Resource, DSPR [29, 30] for five generations under common garden
141 conditions (Fig. 1a) [31]. Several Drosophila community panels in North America, including
142 *Drosophila* Genetic Reference Panel (DGRP) and the *D. melanogaster* Reference Genome,
143 exhibit mosaic genomic ancestry (~20% African, ~80% European) shaped by natural selection

144 against incompatible allele combinations [32]. This can also be expected in DSPR populations,
145 highlighting the need for a genetically diverse population in experimental evolution, as such
146 expanded genotypic diversity would provide a broad substrate for selection facilitating the study
147 of complex traits and adaptation. The properties of the DSPR are described elsewhere [29, 30].
148 From this genetically diverse base population, 36 lines were independently subjected to one of
149 three dietary selection regimes for 65 generations with each regime replicated 12 times in large
150 population cages (N > 4,000 flies; Fig. 1a). One population (N > 4,000) was maintained without
151 selection exposure for the duration of selection. Selection in these populations acted primarily
152 on reproductive success and early-life survival under dietary stress, rather than directly on
153 lifespan. Consequently, differences in longevity observed in the inbred lines likely reflect
154 correlated responses to selection on nutrient-dependent fitness rather than direct selection for
155 extended lifespan.

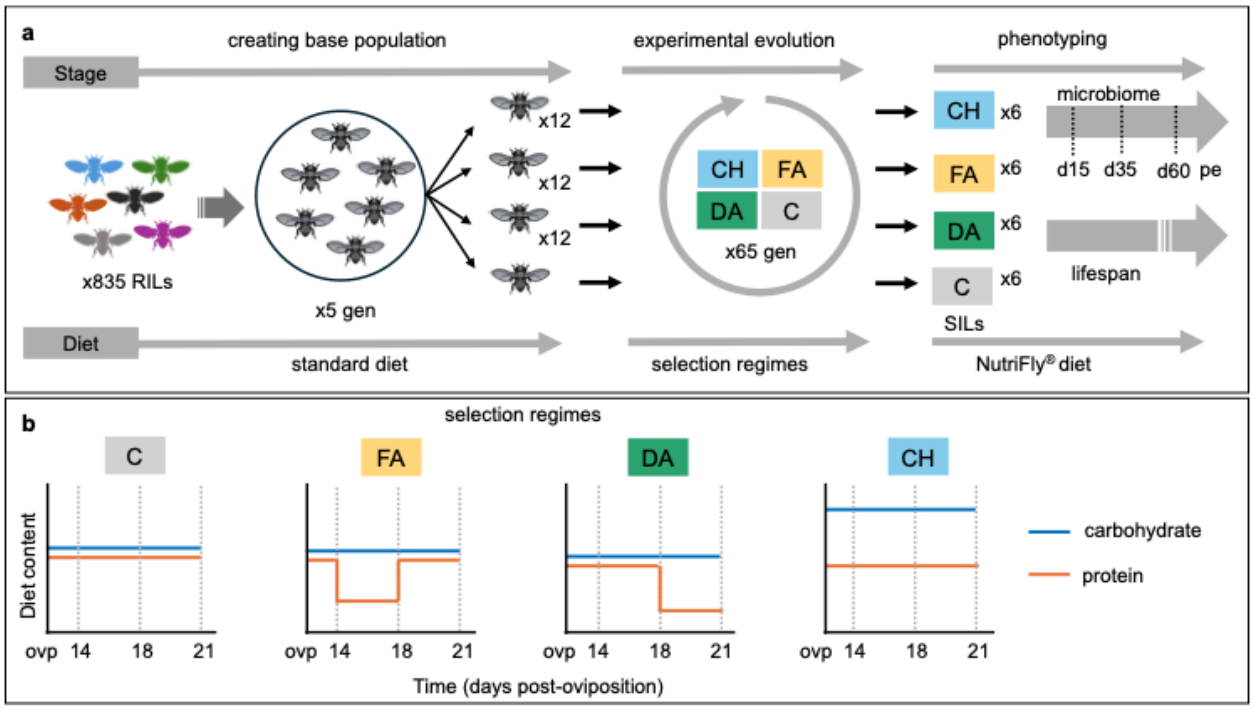


156

157 **Figure 1:** Study design. **a.** A total of 835 recombinant inbred lines of the DSPR rared on
158 standard maintenance diet were interbred into a genetically diverse population and subjected to
159 experimental evolution in four diet treatments for 65 generations. Selection was terminated after

160 65 generations, and flies in each regime inbred in vial replicates, here denoted, *selection inbred*
161 *lines*, or SILs and maintained on common NutriFly diet. Control flies were maintained on
162 standard diet throughout selection in one cage at N > 4,000 and also moved to NutriFly at
163 selection termination. Six SILs per regime were each expanded into 6 replicates, alongside
164 pseudo replicate vials of C flies. Microbiome composition was measured at 15, 35 and 60 days
165 post-eclosion in 3 vial replicates. Survival was measured in a separate set of 3 vials. **b.**
166 Selection regimes: 1) fluctuating (FA), 2) deteriorating (DA) and 3) constant high (CH) nutrient
167 availability were set up in 12 replicate cages (N > 4000 flies per cage) and fed sequences of low
168 protein (LP) and control (C) diet alternations or constant high sugar (HS) diet over a 21-day
169 cycle post-oviposition (ovp) per generation (see methods). Note: DA and FA received temporal
170 alternations of contro and low protein levels; CH received an oversupply of sugar; C was
171 retained on standard diet for the DSPR (no deliberate selection).
172
173 *Nutritional composition of diets constituting selection regimes.* Based on previously published
174 formulations [25, 31, 33], we used three diets that systematically varied in the ratio of protein
175 (yeast) to carbohydrate (sucrose) to impose distinct nutritional selection pressures. Each diet
176 was prepared per liter of water with the following composition: Control diet - 10 g agar, 50 g
177 sucrose**,** 200 g yeast**,** and 2.7 g tegosept (dissolved in 11 mL ethanol); Low-protein diet - 10 g
178 agar, 50 g sucrose, 100 g yeast, and 2.7 g tegosept; High-sugar diet - 10 g agar, 342 g sucrose,
179 200 g yeast, and 2.7 g tegosept. Yeast provided the principal protein source, and sucrose
180 supplied carbohydrates. The control diet yielded an intermediate protein: carbohydrate ratio
181 (P:C ≈ 1 : 0.5) typical of standard laboratory diets that support optimal growth and fecundity.
182 The low-protein diet reduced yeast content by half while maintaining sucrose levels, generating
183 a protein-limited condition (P:C ≈ 1 : 1). The high-sugar diet increased sucrose concentration
184 roughly sevenfold, creating a carbohydrate-rich environment (P:C ≈ 1 : 3). Percent
185 macronutrient content by energy was approximately 45 - 53% protein and 47–52% carbohydrate

186 for the control, 36–41% protein and 59–64% carbohydrate for the low protein diet, and 17–19%
187 protein and 81–83% carbohydrate for high sugar diet.
188
189 *Maintenance of the control population.* Prior to the onset of experimental evolution, the
190 recombinant inbred lines used to generate the base population were maintained on a standard
191 cornmeal–dextrose maintenance diet (40.8 g cornmeal, 21.6 g yeast, 86.3 g dextrose, 6.25 g
192 agar per liter of water, with 1.8 g tegosept). This base diet contained lower protein and
193 carbohydrate levels than any of the experimental diets, ensuring that the defined sugar–protein
194 diets represented clear nutritional shifts.
195
196 To preserve an ancestral baseline for comparison, the unselected control population was
197 maintained throughout the experiment on the cornmeal–dextrose maintenance diet described
198 above - the same diet on which the DSPR founder population was reared prior to the start of
199 selection. We note that this “maintenance” diet differs from the “control (C)” diet used as one of
200 the experimental selection treatments (see above). Using the ancestral diet for the unselected
201 population ensured that these flies represented the pre-selection reference state, avoiding
202 inadvertent selection under any of the experimental diets. The control diet was considered
203 optimal for growth and reproduction and provided a reference for evaluating nutritionally
204 stressful regimes (low protein or high sugar) that impose either limitation or oversupply of key
205 nutrients (previously characterized in Ng’oma et al. [34]).
206
207 *Construction of selection treatment regimes*. From these diets, we designed three selection
208 conditions (Fig. 1b) by alternating the sequence in which the diets were presented to flies in
209 each selection generation. The Fluctuating Availability (FA) treatment alternated nutrient
210 provision as follows: flies received a control until day 14 post-oviposition (po), low protein diet
211 from day 14 - 18 po, and control diet again until day 21 po when eggs were collected to seed

212 the next generation. Flies in the Deteriorating Availability treatment (DA) received a standard
213 diet until day 18 po, followed by a low protein diet until day 21 po, at which eggs were collected.
214 Files in the Constant High sugar treatment (CH) received the high sugar diet throughout, until
215 day 21 po. Alongside selection cages, we maintained one population (N > 4000) that was not
216 exposed to experimental selection and likely remained outbred at the time of this assay, with no
217 observed population bottlenecks and assuming weak genetic drift. Because eggs were collected
218 from survivors at day 21 po each generation, selection acted primarily through differences in
219 fecundity and viability during early adulthood under each dietary regime. Longevity beyond this
220 window was therefore not a direct target of selection but could evolve indirectly as a correlated
221 response to nutrient-dependent reproductive success and stress tolerance. These dietary
222 regimes therefore varied in both macronutrient composition and temporal availability during
223 selection. This may invoke distinct evolutionary responses in the reproduction–survival trade-off.
224 We interpret results with this fact in mind.
225
226 *Selection inbred lines (SILs).* Experimental evolution was performed for 65 generations, after
227 which populations were inbred in replicated vials for each of 36 selection populations at the
228 onset of the Covid pandemic for 38 generations (~19 months). At the end of experimental
229 evolution, all flies were of similar age and sampled from the actively reproducing cohort,
230 ensuring that alleles influencing fecundity and early-life survival were those most consistently
231 transmitted to the next generation. We refer to inbred lines derived from experimental selection
232 as Selection Inbred Lines (SILs, Fig. 1a). SILs were maintained in common garden conditions
233 on a molasses-based Nutri-Fly® diet (Genesee Scientific) until assaying, and the unselected
234 group was held at high population in a cage until assay.
235
236 *Sample collection.* For this study, we selected six random SILs from each selection regime (FA,
237 DA, and CH) along with 12 pseudo replicated vials of the non-selected population. Each

238 selected SIL was expanded over three generations, and three vials each were assigned to
239 microbiome and lifespan estimation assays. Each assay vial was seeded with 24 females and 6
240 males to reduce male mating pressure, which is known to reduce female lifespan in *Drosophila*
241 [34, 35]. This set up minimizes mating-induced costs and allows clearer inference on intrinsic
242 female lifespan differences among selection treatments. Our design therefore yields a reduced
243 male sample in lifespan analysis which we consider in the interpretation of results (i.e., 1,670
244 deaths, 176 censored events for females; 572 deaths, 9 censored events for males). Death
245 events were counted three times per week (Monday, Wednesday, Friday) at which time also a
246 fresh food vial was provided. For the microbiome portion, we assayed only females. Based on
247 our prior study indicating key variability in lifespan and fecundity responses to diet across life
248 phases [36], we collected whole flies at three time points (15, 35, and 60 days po, Fig. 1). At
249 each time point, four females were flash-frozen and stored at -80°C for analysis.
250
251 *Diet sources.* Diets were prepared with inactivated SAFPro Relax + YF 73050 yeast (Lesaffre
252 Yeast Corp., Milwaukee, USA), stored at 4°C, and used within 14 days. Evolved lines were held
253 on a common Nutri-fly molasses formulation (Genesee Scientific) based on a Bloomington
254 Drosophila Stock Center Nutri-fly molasses protocol (12.4 g/L yeast, 61.3 g/L yellow cornmeal,
255 and 75.2 ml/L molasses). This change was necessitated by shortages in supplies during and
256 after the pandemic. Across all assays, flies were maintained in a temperature-controlled
257 chamber at 23°C under continuous light, mirroring conditions under which the DSPR was
258 originally generated and maintained [29]. Flies were supplied with fresh food three times per
259 week (Monday, Wednesday, Friday).
260
261 16S rRNA amplicon sequencing
262 Whole-fly 16S rRNA sequencing without surface sterilization captures both internal and surface-
263 associated microbes and thus represents the total host-associated microbiome. This approach

264 aligns with our goal of characterizing microbiome responses to long-term dietary selection at the
265 whole-organism level. All samples were reared on a common diet medium prepared in bulk and
266 distributed across all selection lines, ensuring a shared environmental microbial background.
267 Therefore, observed differences across selection treatments likely reflect evolved host-
268 microbiome associations rather than environmental contamination. DNA was extracted from
269 pools of two to four flies using the Qiagen DNeasy Blood & Tissue Kit (Cat. No 69504). Samples
270 were manually homogenized with a glass pestle in ATL buffer, incubated for 4 hours, and
271 processed following the kit manufacturer's protocol. DNA yield and quality were assessed using
272 a nanodrop spectrophotometer (ND-1000) and Qubit 4 Fluorometer with the Qubit 1X dsDNA
273 HS Assay Kit (Cat. No Q33231). Samples were normalized as needed with elution buffer and
274 sequenced on a MiSeq instrument (PE250-v2 Nano flow cell, 25 cycles) targeting the V4 region
275 of the bacterial 16S rRNA gene with primers 515F (5'-GTGCCAGCMGCCGCGGTAA-3') and
276 806R (5'-GGACTACHVGGGTWTCTAAT-3') [37, 38]. Sequencing was performed at the
277 University of Missouri Genomics Technology Core.
278
279 Data Analysis
280 *Lifespan*. We first explored and compared survival patterns among selection regimes in a total
281 of 2,427 individuals (2,242 deaths, 185 censored), using survival models that included sex
282 either as a covariate or in sex-stratified analyses. Kaplan-Meier survival curves indicated
283 marked sex differences in survival probability (Additional File 2 Table S1) and changes in the
284 relative survival rankings of selection regimes over time. Because each selection regime (CH,
285 DA, FA) consisted of multiple unique selection inbred lines (SILs) replicated across vials, our
286 design required modeling fixed effects of regime, sex, and their interaction, while accounting for
287 random effects of SIL and vial.
288

To evaluate the effects of dietary regime and sex on survival, we fitted mixed-effects Cox proportional hazards models with a random intercept for SIL nested within vial. We compared an additive model (`event ~ regime + sex + (1 | SIL/vial)`) and an interaction model (`event ~ regime * sex + (1 | SIL/vial)`) using ΔAIC as the comparison criterion. Proportional hazards assumptions were tested using Schoenfeld residuals. All fixed effects (regime, sex, and their interaction) significantly violated this assumption ($\chi^2$ test, $p < 0.01$), indicating time-varying hazard ratios. A time-transformed Cox model (`regime + tt(sex)`, where `tt(x) = x * log(t)`) improved fit (ΔAIC = 15.6), confirming time-dependent effects of sex.

Given these violations and the hierarchical structure of our data, we proceeded with a discrete-time survival framework. We implemented a generalized linear mixed model (GLMM) with a complementary log–log (cloglog) link using **lme4**, specifying event ~ regime * sex + (1 | SIL). This model structure best fit the data (ΔAIC = 17, $p = 2.7 \times 10^{-5}$), while additional vial-level random effects did not improve fit (ΔAIC = +2).

To confirm robustness, we re-estimated the same model using a fully Bayesian hierarchical approach implemented in **brms**, specifying identical fixed and random effects and a cloglog link. Weakly informative priors were applied (normal(0, 2) for fixed effects; Student-t(3, 0, 2.5) for random effects). Results from both approaches were concordant, and the Bayesian model was used for inference and visualization. Full model specifications and diagnostics are provided in Additional File 1.

Our recent study testing effects of larval nutrition on adult phenotypes in this population [36] showed that patterns of survival can vary significantly across shorter periods of time in adult

314 lifespan. To understand evolved patterns of survival in each selection treatment, we examined
315 percentile survival differences in ten-day intervals in which each of our sampling time points for
316 the microbiome portion (described next) formed the median: 10-20, 30-40, and 55-65 days, post
317 eclosion. We tested for significant differences between treatments in each time interval I1, I2
318 and I3 using either analysis of variance (Anova) or Kruskall-Wallis tests followed by an
319 appropriate post-hoc test (Turkey's HSD or Dunn's Test).
320
321 *Microbiome analysis*: We processed Illumina reads using the R library DADA2 pipeline [39],
322 leveraging its use of Amplicon Sequence Variants (ASV), an alternative to Operational
323 Taxonomic Units (OTUs) that enables the detection of single-nucleotide differences in amplicon
324 sequencing and avoids the limitations of traditional OTU clustering by using exact biological
325 sequences. Reads were quality-filtered and trimmed at positions 225 (forward) and 200
326 (reverse), and chimeras were removed. Taxonomy was assigned using the Silva database
327 (v138.1). Samples with fewer than 200 reads after sequence merging were excluded. We
328 investigated the proportion of reads identified as *Wolbachia* and found that these constituted
329 less than 1% reads in the entire data set (Additional File 3, Fig. S7). Prior to analysis, these
330 reads were removed as common practice [40]. We performed mainstream analysis and
331 visualization using the R library **phyloseq** [41]. Read counts were normalized using a log-
332 transformation: `log(1 + x)/sum(log(1 + x))`. This approach combines two commonly used
333 normalization equations, log(1 + x) and (x)/sum(x), into one step and effectively scales data to
334 relative abundances (i.e., the proportion of specific microbial groups within samples) while
335 revealing differences in rare taxa through its log transformation [42–44]. This method was used
336 instead of rarefication because rarefication is known to unnecessarily discard samples and to
337 have a higher false positive rate (McMurdie and Holmes 2014).
338

339 We assessed microbiome diversity using both alpha and beta diversity metrics. For alpha
340 diversity, we calculated Shannon and observed species indices from non-normalized sequence
341 data, as standard practice to preserve true richness and evenness without introducing artifacts
342 from normalization. Beta diversity was also evaluated on a full data set using principal
343 coordinate analysis (PCoA) based on UniFrac distances, with phylogenetic trees generated via
344 the *ape* package [45]. To test for overall differences in microbial community structure across
345 treatments and time points, we applied permutational multivariate analysis of variance
346 (PERMANOVA) using the **vegan** R package [46], applying Bonferroni correction to control for
347 false positives. We further used PERMDISP2, a multivariate analogue of Levene's test [47], to
348 determine whether observed differences were influenced by dispersion within groups.
349 Collectively, these analyses provided a robust framework for understanding the drivers of
350 microbial community composition in our study.
351
352 To identify taxa associated with specific selection treatments or age groups, we performed
353 Indicator Species Analysis using the **indicspecies** R package [48]. Based on the ASV table, we
354 assessed associations between microbial taxa and either selection treatment or fly age.
355 Indicator values were calculated using the `multipatt()` function, which evaluates both
356 specificity and fidelity of taxa to groups, and statistical significance was assessed using 999
357 permutations.
358
359 To assess whether microbiome composition could predict fly age, dietary regime, or their
360 interaction, we implemented a predictive random forest model adapted from [49]. Using the
361 **caret** R package, we trained models to classify samples based on time point, treatment, and
362 their combination, accounting for each unique vial and treatment-age group. Model performance
363 was evaluated using repeated five-fold cross-validation, repeated five times. To account for
364 variability in accuracy estimates, we ran 100 model iterations and calculated the mean

predictive accuracy for each classification task. Additionally, we extracted the top 15 most important taxa contributing to each model, based on feature importance scores from the trained random forest classifiers.

## Results

### Overall longevity following diet selection

Lifespan performance in the non-selected base population (C) served as a benchmark for evaluating selection treatments (Fig. 2). Summary survival patterns are presented in (Additional file 2, Table S1). Overall, a log-rank test comparing survival across selection regimes revealed highly significant differences in lifespan ($\chi^2 = 274$, df = 3, $p < 2e{-}16$). CH (i.e. constant high sugar) flies showed markedly lower survival (Fig. 2a-c), with far more deaths than expected under the null hypothesis of equal survival curves (median 27 days vs 42 days in C; Additional File 1, Table S2). In contrast, DA and FA (i.e. deteriorating- and fluctuating-availability) flies exhibited higher-than-expected survival (median 41 and 37 days, respectively). The control group lived the longest, significantly exceeding both CH (p = 5.91e-09) and FA (p = 0.0273) regimes (Fig. 2a). These patterns are reflected when survival is analyzed within 10-day bins around microbiome sampling time points, with the CH showing steeper mortality (Fig. 2c).

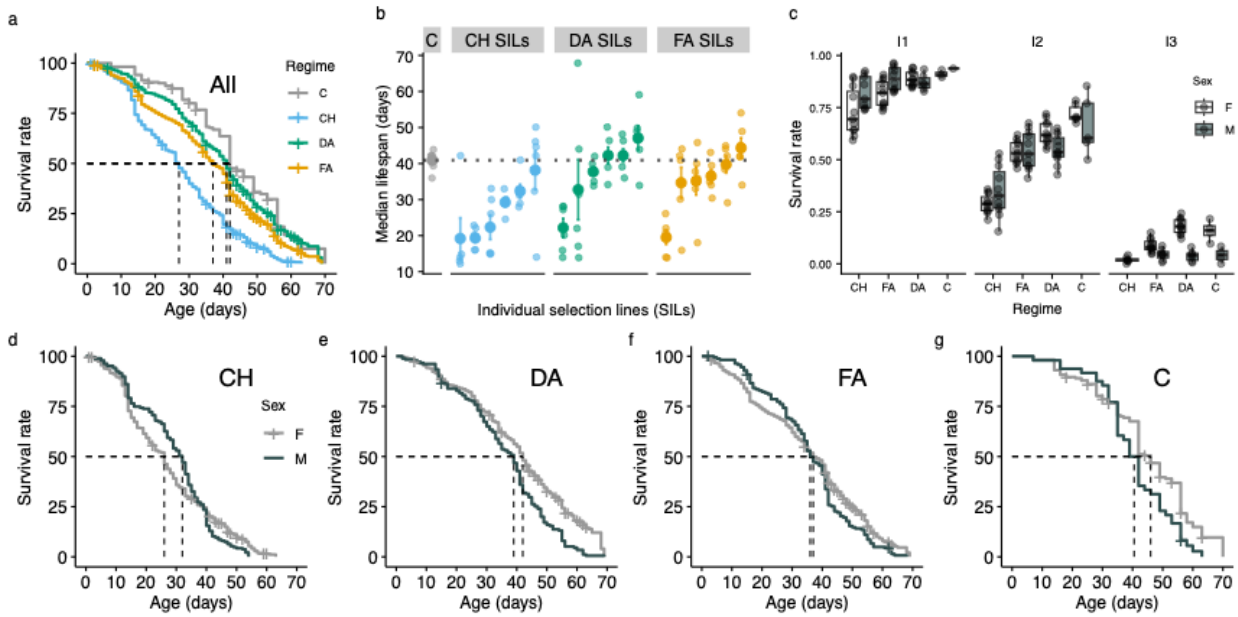


**Figure 2:** Survival performance: **a.** overall with both sexes together, **b.** median survival in each selection group of SILs, **c.** survival by sex based on bins of 10 days in which the sampling time point (of the microbiome) is the median (only bins containing assayed time points of 15, 35 and 60 days are shown (I1=10-20 days, I2=30-40 days, I3=55-65 days); **d-g**, comparison of sex performance averaged across SILs in each selection treatment.

Sex-specific survival patterns

Sex differences in lifespan were apparent across all selection regimes. A Cox proportional hazards model with a time-varying effect of sex revealed significant differences in survival across regimes ($\chi^2$ = 304.8, *df* = 4, $p$ < 2e-16). Flies from the constant high-sugar regime (CH) had the highest risk of death (HR = 2.68, 95% CI: 2.28–3.15, $p$ < 2e-16), followed by the fluctuating-availability (FA) regime (HR = 1.49, 95% CI: 1.27–1.75, $p$ = 9.9e-07). The deteriorating-availability (DA) regime showed a modest, borderline effect (HR = 1.17, 95% CI: 1.00–1.38, $p$ = 0.055). The time-varying term for sex, *tt(Sex_binary)*, was also significant (HR = 1.10, 95% CI: 1.06–1.13, $p$ = 2.9e-10), indicating that the sex effect on mortality increased with age (Additional File 3 Fig. S1c). Males thus faced progressively higher mortality risk than

399 females over time. Together, these results demonstrate that long-term selection under stressful
400 dietary regimes, particularly constant high sugar, led to pronounced lifespan reductions, with
401 sex-specific differences in mortality risk that intensified with age.
402
403 Although sex differences were clear, their magnitude and direction varied (Fig. 2d-g). In the
404 control population, females outlived males, with median lifespans of 46 and 40.5 days,
405 respectively (95% CI for females: 42 - 49; males: 35 - 44). A similar, though smaller, sex gap
406 was observed under the DA regime (median: females 42, males 39 days). In the FA regime,
407 survival differences between sexes were minimal, with overlapping confidence intervals and
408 near-identical medians (females: 37 days, males: 36 days). Interestingly, under the CH regime,
409 males lived slightly longer than females, with median lifespans of 32 vs 26 days. Generally, CH
410 and FA treatments favored male survival earlier, reversing later in life with higher female
411 survival (Fig. 2c, d, f). Conversely, DA and C regimes showed greater female survival through
412 most of life (Fig. 2c, Fig. 2e,g, Additional file 3 Fig. S1 - S2), suggesting adjustment to dietary
413 stress through reduced early mortality (DA, FA) or combined early and late-life mortality
414 reduction (DA, C). These results indicate that selection regime influences not only overall
415 lifespan but also modulates sex-specific survival patterns, with a marked sex-based lifespan
416 reversal occurring under constant high sugar (CH). Results further suggest that dietary stress
417 adaptation might involve distinct survival strategies in this population, with DA and FA regimes
418 prioritizing early-life resilience and DA further extending late-life survival.
419
420 Interactive impacts of sex and diet regime
421 Relative to C flies, the DA and FA regimes showed reduced early mortality (in I1 and I2, Fig. 2c)
422 favoring longevity, but diverged later (in I3), with FA experiencing slightly higher late mortality
423 while DA maintained slower rates. Control flies exhibited the lowest mortality in the first half of
424 lifespan (I1 and I2). In contrast, CH flies suffered heavy mortality across the entire curve.

425 Underlying these differences are apparent rank changes in female vs male curves suggesting
426 strong regime by sex interactions in survival (Fig. 2d-g). To evaluate the effects of selection
427 regime, sex, and their interaction on mortality risk over time, we fit both Bayesian and
428 frequentist generalized linear mixed models (GLMMs) using a complementary log-log link.
429 Estimates from both approaches were highly consistent, showing strong effects of time and the
430 CH selection regime on increased mortality probability, while the DA and FA regimes had
431 weaker or non-significant effects (Table 1, Fig. 3, Additional file 3 Fig. S3-S5). Male flies
432 experienced a modestly elevated risk overall, and these differences were most pronounced in
433 the CH treatment (Fig. 3). Bayesian posterior direction (PD) values further supported the
434 robustness of key effects (e.g., time, CH, FA, Male, and CH : Male), with >96% of posterior
435 samples in the direction of the mean. Full model estimates are provided in Table 1.
436
437 Predicted probabilities of death varied by selection regime and sex in both Bayesian and
438 frequentist GLMMs (Additional File 3 Fig. S3, S4, S6). In C flies, females showed the lowest
439 mortality probability (~1%), while CH females had the highest (~3–4%), with overlapping
440 estimates between models. Males consistently exhibited higher predicted risks than females
441 within most regimes, particularly under DA and FA. Both models revealed minimal sex
442 differences in CH, where female and male predictions were comparably elevated. These
443 adjusted predictions support the significant regime and sex effects identified in the full models.
444
445 **Table 1.** Comparison of Bayesian and frequentist estimates from generalized linear mixed
446 models (GLMMs) assessing the effects of selection regime, sex, and time (standardized week)
447 on the probability of mortality. Bayesian estimates are posterior means with 95% credible
448 intervals and posterior direction (PD), while frequentist GLMM estimates are shown with
449 standard errors (SE), z-values, and associated p-values. The reference levels are the base
450 population (C) and females.

451

| Effect | Bayesian estimate (95% CI) | PD direction (%) | glmer estimate (se) | z-value | p-value |
|---|---|---|---|---|---|
| Intercept | -4.53 (-4.83, -4.23) | 100 | -4.54 (0.14) | -32.23 | < 2e-16 |
| Week (z) | 0.89 (0.85, 0.93) | 100 | 0.89 (0.02) | 40.39 | **< 2e-16** |
| CH | 1.21 (0.75, 1.67) | 100 | 1.23 (0.21) | 5.82 | **5.9e-09** |
| DA | 0.09 (-0.37, 0.56) | 65.4 | 0.11 (0.21) | 0.51 | 0.6084 |
| FA | 0.45 (-0.01, 0.93) | 97.2 | 0.47 (0.21) | 2.21 | **0.0273** |
| Male | 0.33 (-0.01, 0.67) | 96.7 | 0.35 (0.17) | 2.04 | **0.0416** |
| CH : Male | -0.47 (-0.84, -0.09) | 99.0 | -0.49 (0.19) | -2.55 | **0.0109** |
| DA : Male | 0.12 (-0.25, 0.53) | 73.4 | 0.10 (0.20) | 0.52 | 0.6007 |
| FA : Male | -0.14 (-0.51, 0.26) | 75.4 | -0.16 (0.20) | -0.81 | 0.4210 |

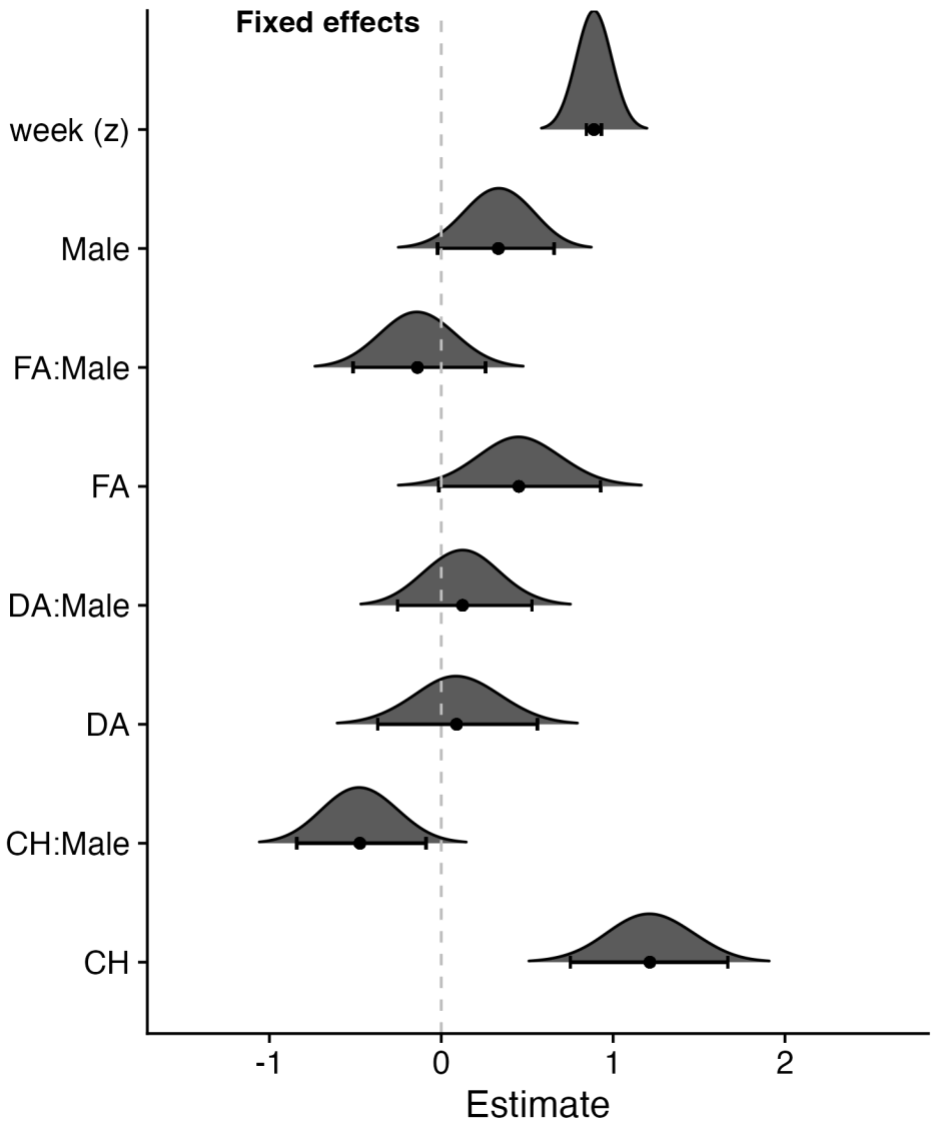


**Figure 3:** Fixed effects from hierarchical modeling of survival. Posterior distributions and 95% credible intervals (CIs) for fixed effects from the Bayesian model. Each ridge represents the estimated posterior distribution of a model coefficient. Points indicate posterior medians, and horizontal bars show 95% CIs. Vertical dashed line denotes the null effect (0). Parameters include treatment effects (CH, DA, FA), sex (Male), and their interactions, relative to the reference group (females in the control C regime). Estimates are on the scale of the linear predictor.

461 Microbial composition across selection regimes and time points

462 To assess microbial composition, we first analyzed the average relative abundance of phyla
463 across time points and selection regimes (Fig. 4). Overall, all selection regimes (CH, DA, FA)
464 displayed broadly similar microbial compositions that were distinct from the control, primarily
465 due to lower Proteobacteria abundance and higher Firmicutes at the initial time point. Over time,
466 Proteobacteria steadily increased across all treatments, ultimately converging between 45–65 %
467 by T2. Other phyla, including Actinobacteria, Bacteroidota, and Fusobacteriota, were more
468 abundant in the selected regimes than in controls but generally declined with age (Additional file
469 3: Fig. S8c–e).

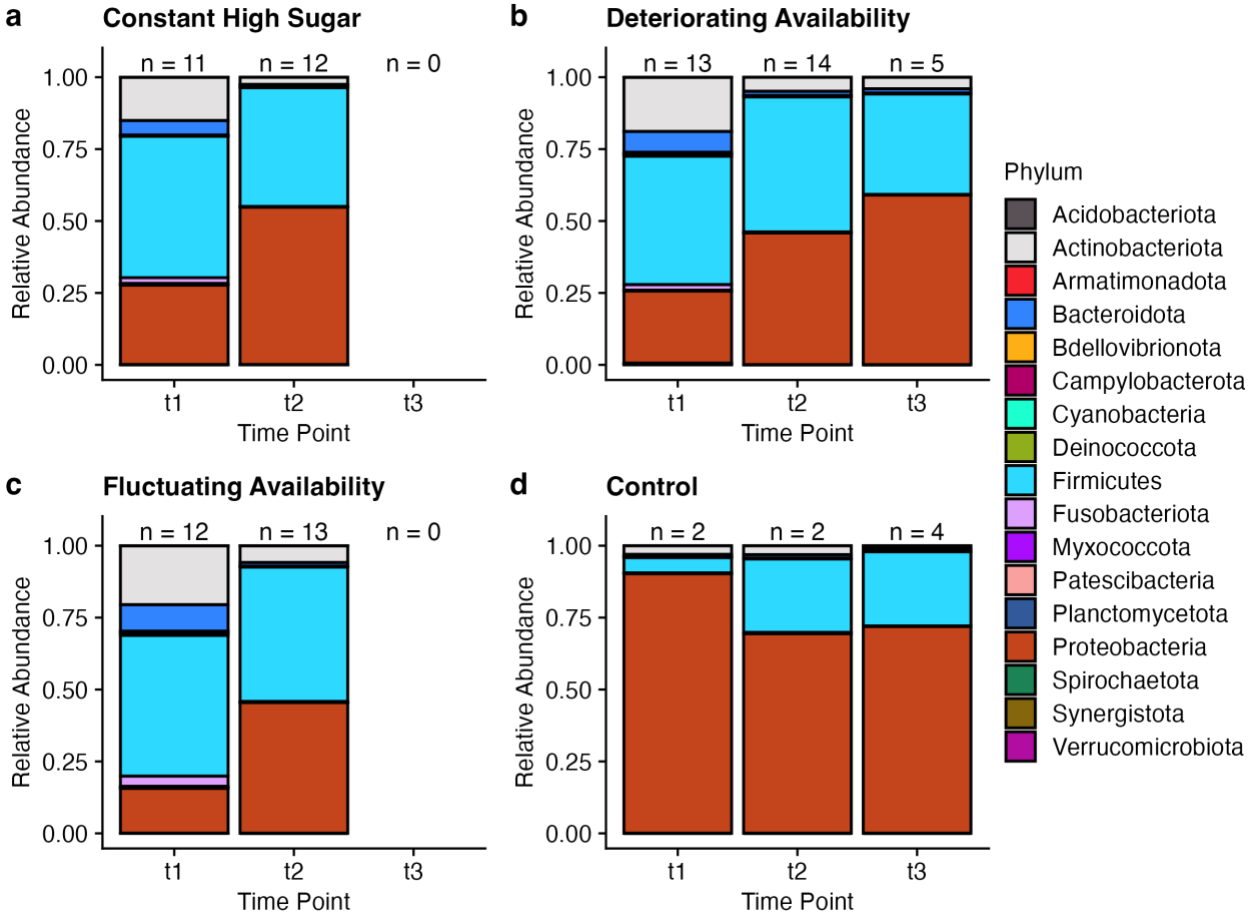


470

471 **Figure 4:** Phylum-level relative abundance of bacterial communities across timepoints and

472 dietary treatments. Stacked bar plots show the log-transformed relative abundance of bacterial
473 phyla at three timepoints t1, t2 and t3 (i.e. 15, 35, and 60 days post-eclosion) within each dietary
474 treatment: **a.** constant high sugar (CH), **b.** decreasing nutrient availability (DA), **c.** fluctuating
475 nutrient availablity (FA), and **d.** control non-selected group (C). Each bar represents the mean
476 relative abundance of samples collected at a given timepoint (n indicated above each bar).
477 Colors correspond to bacterial phyla, as shown in the shared legend.

478 To explore compositional significance of observed relative abundance dynamics, we performed
479 an indicator species analysis (ISA) at both the genus and species level. At the species level, an
480 indicator species analysis (ISA) identified 35 species differing across time points, 5 across
481 selection regimes, and 18 across both factors. Most time-related species (81 %) were enriched
482 at the earliest time point (T1), highlighting pronounced early-life microbiome restructuring.
483 Control samples were enriched in three *Acetobacter* species (*A. aceti*, *A. oryzifermentans*, and
484 *A. tropicalis*), whereas *Corynebacterium amycolatum* and *Mobiluncus curtisii* (Actinobacteria)
485 were associated with CH and FA, respectively (Table 2). Several species were linked to specific
486 combinations of diet and time. Notably, the genus of core Drosophila gut colonizers,
487 *Acetobacter,* were depleted in the selected lines but present across all time points in controls,
488 indicating that long-term dietary selection disrupted the *Acetobacter*-dominated microbiome
489 characteristic of non-selected flies. The full output of the ISA looking across time point and
490 selection regime can be found through (Additional file 4).

491

492 At the genus level, ISA identified 39 genera differing across time points, 8 across selection
493 regimes, and 28 across both factors (Additional file 2 Table S2). Among the diet-associated
494 genera, *Fructilactobacillus* (Firmicutes) was enriched in CH; *Mobiluncus* (Actinobacteria) and
495 *Pelomonas* (Proteobacteria) in FA; *Leptotrichia* (Proteobacteria) in CH + FA; *Acinetobacter*

496 (Proteobacteria) in DA + FA; and *Actinomyces* (Actinobacteria), *Neisseria* (Proteobacteria), and
497 *Lacticaseibacillus* (Firmicutes) in CH + DA + FA. Together, these results indicate that dietary
498 selection history reshaped both phylum- and genus-level composition, resulting in distinct,
499 convergent microbiomes among selected lines that diverged from the control.
500
501 Based on prior studies linking microbial composition to immune function [50, 51], we
502 hypothesized that Proteobacteria and Firmicutes could influence hosts positively or negatively
503 depending on their relative proportions. We calculated phyla ratios as age-specific indicators of
504 treatment effects (Additional file 3 Fig. S8f-g). In the selection regimes, the Proteobacteria-
505 Firmicute ratio generally increased over time (Additional file 3 Fig. S8f), while the Bacteriodota-
506 Firmicute ratio decreased between T1 and T2 but then increased in DA between T2 to T3
507 (Additional file 3 Fig. S8g). The control group began with higher ratios than the treatments and
508 exhibited a general decline, suggesting an age-related increase in Firmicutes relative to
509 Proteobacteria and Bacteriodota. These patterns reveal contrasting dynamics between
510 Proteobacteria and Bacteroidota that are influenced by Firmicutes.
511
512 Table 2: Species-level enrichment across time and selection regime.

| **Species** | **Time point** | **Regime** | **Remark** |
|---|---|---|---|
| *Acetobacter aceti* | T1, T2, T3 (C) | C only | Core gut colonizer; disrupted in treatments |
| *Acetobacter oryzifermentans* | T3 (DA), all time points (C) | C, DA | Found in fermented substrates |
| *Acetobacter tropicalis* | T3 (C) | C only | Common hindgut colonizer |
| *Acetobacter persici* | T1 (C, CH, DA), T2 (all), T3 (C, DA) | Mixed | Broad presence but absent in FA at later time points |

| | | | |
|---|---|---|---|
| *Corynebacterium amycolatum* | - | CH | Treatment-associated species |
| *Mobiluncus curtisii* | - | FA | Treatment-associated species |

513

514

515 **Microbial diversity dynamics and predictive modeling**

516 We assessed microbial diversity across time points and dietary selection treatments using both
517 alpha and beta diversity metrics. At the ASV level, both observed richness (Fig. 5a) and
518 Shannon index (Fig. 5b), shifted significantly between T1 and T2 in all selection regimes,
519 particularly in DA and FA indicating substantial early-life microbial restructuring. Some
520 differences persisted into T3 in DA, although CH and FA lacked T3 data due to shortened
521 lifespans. Similar patterns were observed at the genus- evel (Fig. 5c-d). Beta-diversity analyses
522 (PCoA and PERMANOVA) revealed significant effects of time point, selection regime, and their
523 interaction ($p = 0.001$), with pairwise contrasts showing pronounced T1 to T2 shifts in DA and
524 FA (Fig. 6b-c). Dispersion tests further supported temporal changes within treatments,
525 especially in DA and CH, and early compositional divergence between control and selected
526 lines. Overall, age exerted a stronger influence than dietary regime on microbial community
527 structure.

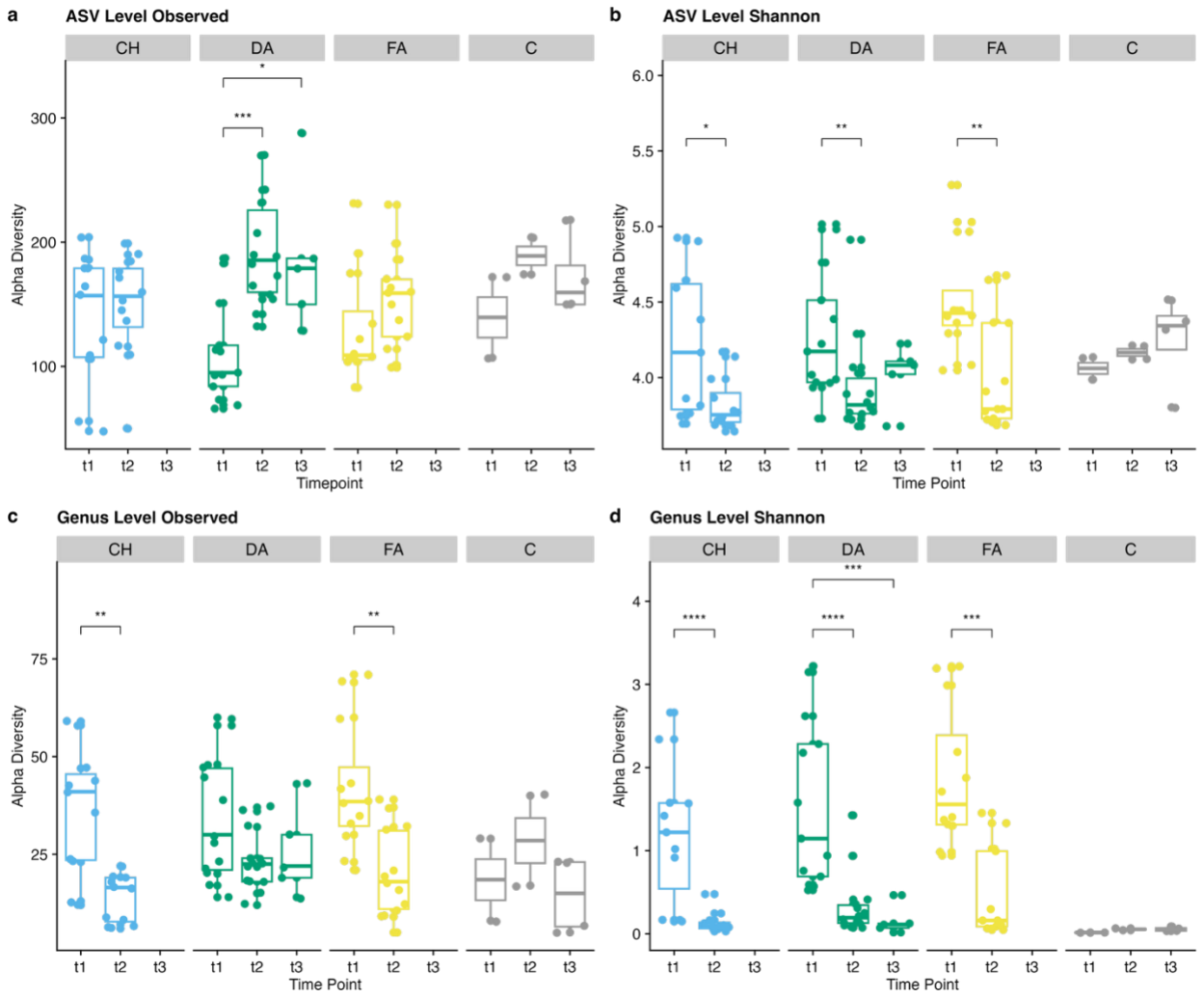


528

529 **Figure 5:** Temporal changes in microbial alpha diversity across dietary treatments(CH, DA, FA

530 and C) at ASV (a-b) and genus (c-d) levels. **a&c** are observed diversity while **b&d** are Shannon-

531 Weiner index. Significance between timepoints is from pairwise Wilcoxon rank-sum tests ($p <$

532 $0.05$), using raw p-values. Timepoints t1, t2 and t3 are 15, 35, and 60 days post-eclosion.

533

534 To evaluate the predictive value of microbial profiles, we trained random forest models to

535 classify age, selection regime, and their interaction (Additional file 3 Fig. S10). The model

536 predicting time point achieved the highest accuracy (78.8 %), identifying *Acetobacter persici*,

537 *Cutibacterium acnes*, and *A. oryzifermentans* as key predictors. Models predicting dietary

538 regime or the time x regime interaction performed less accurately (40.1 % and 32.2 %,

539 respectively), likely reflecting limited sample sizes in the control and T3. Across all models, *A.*

540 *persici* consistently emerged as a strong age-associated taxon, increasing in abundance in

541 older flies across regimes.

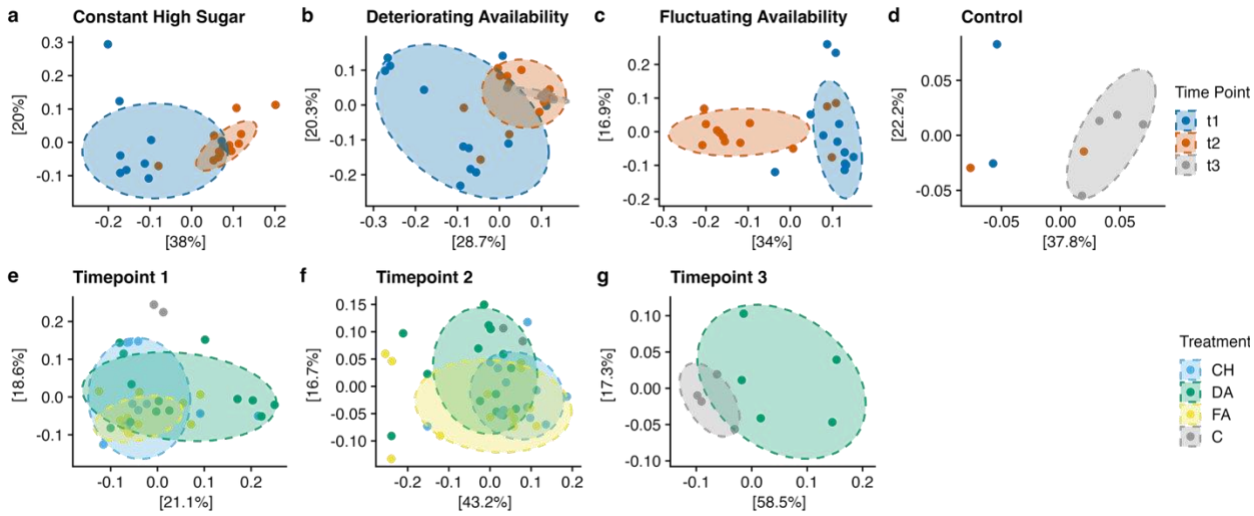


542

543 **Figure 6:** PCoA showing species diversity of dietary regimes over time (a - d) and across

544 regimes at each timepoint (e - g). **a.** constant high sugar (CH), **b.** decreasing nutrient availability

545 (DA), **c.** fluctuating nutrient availability (FA), **d.** control non-selected group (C), **e.** 15 days post

546 eclosion (dpe) (T1), **f.** 35 dpe (T2), and **g.** 60 dpe (T3). CH and FA groups did not reach t3,

547 hence no comparisons for T3 for a, c, and g. UniFrac distances are used as beta-diversity

548 metric.

549

550 Given its prominence in both random forest and indicator species analyses, we examined

551 *Acetobacter* abundance in greater detail (Fig. 7). *A. persici* was the most abundant species

552 across regimes, followed by *A. aceti* and *A. oryzifermentans*. From T1 to T2, *A. persici*

553 increased significantly across all selected regimes but not in controls, while *A. aceti* rose in DA

554 and FA. Between treatments, *A. aceti* differed significantly from controls in both T1 and T2, and

555 *A. oryzifermentans* showed broader regime-specific differences. Together, these results indicate

556 that age-related microbial shifts, dominated by *Acetobacter* taxa, are more consistent and

557 predictable than those driven by dietary selection history. However, persistent differences in
558 these core taxa between control and selected regimes suggest that long-term dietary selection
559 also left distinct microbial legacies shaping community composition across ages.

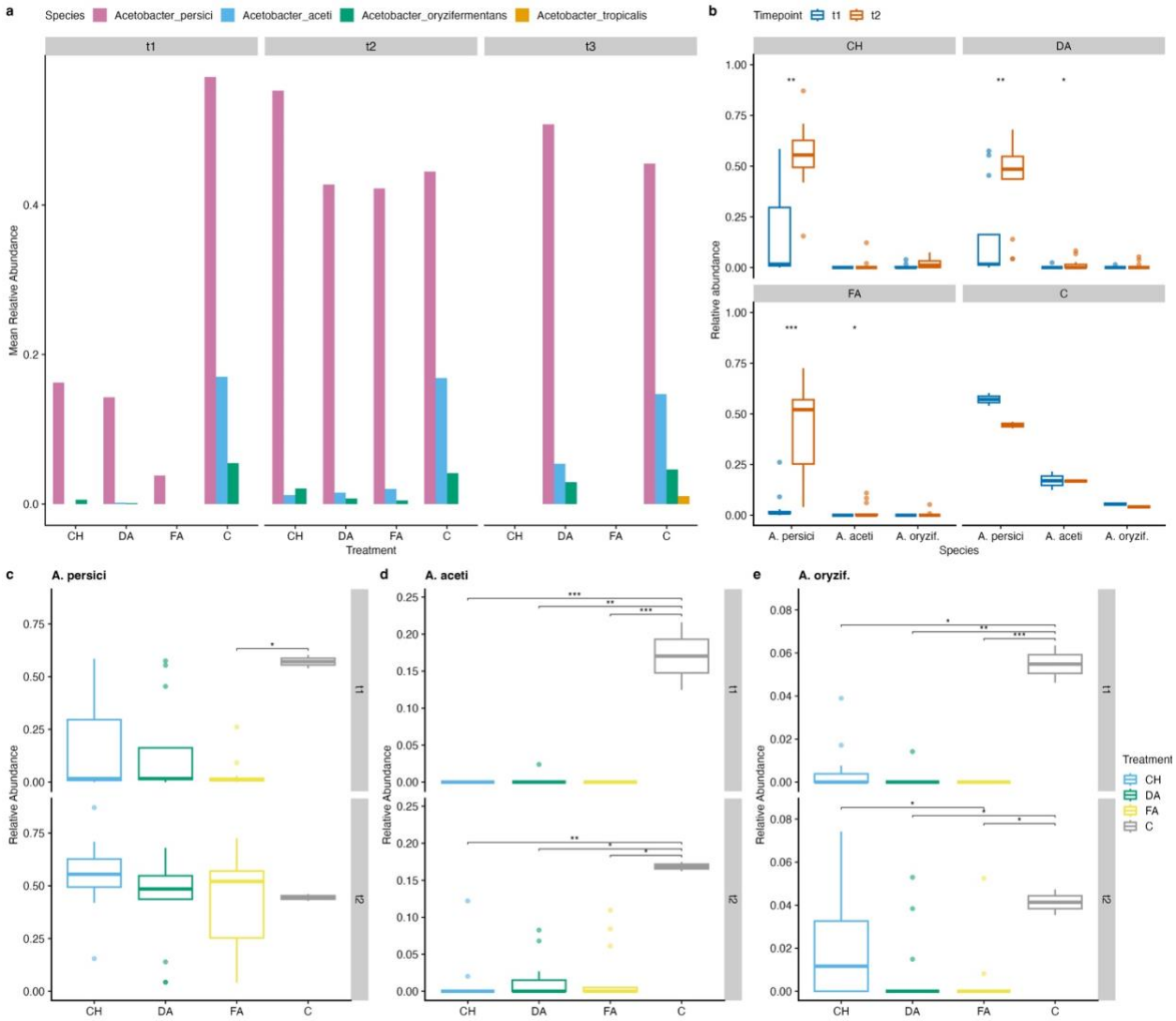


560

561 **Figure 7:** Prevalence of various Acetobacter species across samples: **a.** overview of the
562 average relative abundance of four different acetobacter species. **b.** change in abundance of
563 each species between 15 dpe (T1) and 35 dpe (T2) of each dietary regime. **c-e**. differences
564 between dietary regimes in **c.** *A. aceti*, **d.** *A. persici*, and **e.** *A. oryzifermentans* at both T1 and
565 T2. **b-e**. p-values from Wilcoxon ranked-sum tests.

566 **Discussion**

567 We investigated how long-term dietary selection and inbreeding histories affect survival and
568 microbial community dynamics in *Drosophila melanogaster*. To do so, we used individual diets
569 we have characterized earlier in the DSPR (i.e. high sugar, reduced yeast, and standard diet)
570 [31, 52, 53] to construct selection conditions, DA, FA and CH. While none of the selected lines
571 outperformed the control in lifespan, DA (decreasing protein) selection, representing repeated
572 exposure to a high-to-low dietary environment, produced lifespan performance comparable to
573 the control group after 65 generations. In contrast, flies from FA and CH selection regimes
574 exhibited reduced lifespan when maintained on the standard diet. This pattern indicates that
575 chronic exposure to specific dietary stressors can leave lasting physiological and microbial
576 legacies on lifespan, even after long-term rearing in a common environment. These findings
577 extend our prior work and highlight that historical nutritional stress can generate enduring, and
578 sometimes maladaptive, consequences for longevity.
579
580 **Longevity and sex-specific responses to dietary selection regimes**
581 Among selection regimes, the constant high-sugar (CH) lines showed the strongest survival
582 cost, particularly in females. Rather than indicating incomplete adaptation, this likely reflects a
583 persistent metabolic legacy of chronic sugar exposure, which may influence host–microbe
584 interactions. Prolonged selection under carbohydrate-rich conditions may have reinforced
585 physiological priorities toward nutrient storage and reproduction at the expense of somatic
586 maintenance, leading to reduced lifespan when flies are maintained on a more balanced diet
587 [54, 55]. The pronounced early mortality in CH females suggests carryover effects of metabolic
588 dysregulation during peak reproductive activity, consistent with sugar-induced insulin resistance
589 observed in experimental evolution studies (e.g., [56]).
590 By contrast, lines exposed to fluctuating or deteriorating availability (FA and DA) exhibited more
591 moderate declines, potentially reflecting historical exposure that promoted metabolic flexibility or
592 resilience to nutrient variation rather than chronic abundance. In these lines, survival during

593 early adulthood (a key reproductive window) was maintained, whereas later mortality increased,
594 suggesting trade-offs in resource allocation between reproduction and maintenance.
595
596 Notably, sex-specific patterns emerged: FA males lived longer than females early in life,
597 possibly facilitating sustained mating at a cost to female survival, while in DA a mildly opposite
598 pattern was observed, consistent with maternal investment being favored under limited protein
599 supply. Given that our data focus on longevity patterns rather than a complete set of life-history
600 traits, we interpret these findings as reflecting evolved differences in physiological maintenance
601 rather than comprehensive life-history dynamics. Further, although mutation accumulation is a
602 theoretical factor influencing survival differences, it is unlikely to explain our results. The 65
603 generations of directional selection in large populations would have efficiently purged
604 deleterious alleles. Thus, the observed survival differences more plausibly reflect evolved
605 physiological adjustments to historical nutritional regimes rather than stochastic accumulation of
606 mutations. Overall, the results point to divergent physiological trajectories rooted in past dietary
607 environments, with lasting effects on survival even under a standardized diet.
608
609 Microbiome responses to selection
610 Selection regimes also produced distinct microbiome profiles, representing the primary and
611 most robust evidence of persistent effects of dietary selection. Compared to the control group,
612 selected lines exhibited increased microbial richness and altered taxonomic composition,
613 particularly early in life. The control flies maintained lower Firmicutes and higher Proteobacteria
614 in early adulthood, consistent with a more beneficial, stable microbiome previously associated
615 with greater lifespan in *Drosophila* [57, 58]. Selected lines experienced early colonization by
616 taxa such as *Corynebacterium* and *Mobiluncus*, which in other systems include opportunistic or
617 inflammation-associated species [16, 59, 60]. Studies in both flies and mammals show that early
618 microbiota disruptions can impair host immunity and longevity [12]. These findings suggest that

619 historical dietary stress can imprint persistent effects on microbiome assembly, potentially
620 compromising host survival persistently after the selective pressure is withdrawn. The DA (and
621 to a lesser degree, FA) lines, which maintained more survivors into later life, also showed
622 similar dynamics in microbial composition across age. This is consistent with work showing that
623 early adult microbiome establishment is critical for later-life health in flies [59, 61]. The ability to
624 maintain beneficial taxa may therefore represent a retained trait from prior selection rather than
625 ongoing adaptation in stressful nutritional environments.
626
627 We also detected consistent reductions in beneficial microbial taxa between the control and
628 selection treatments in both T1 and T2, particularly in two core *Acetobacter* species: *A. aceti*
629 and *A. oryzifermentans*. As members of the acetic acid bacteria group, *Acetobacter* species are
630 integral to the fruit fly microbiome and have been linked to critical host functions, including
631 growth and development, insulin signaling, lipid metabolism, and stem cell activity [62, 63]. In
632 our study, flies from the selection regimes exhibited lower relative abundances of these
633 microbes, suggesting that nutritional stress and inbreeding histories may have disrupted the
634 core microbiota. Such disruptions could impair physiological processes and contribute to
635 microbial imbalance and reduced survival. Interestingly, although *A. aceti* has been previously
636 associated with shorter lifespan in *D. melanogaster* [64], we observed the highest levels of *A.*
637 *aceti* and the longest lifespan in control flies. This contrast may reflect context-dependent
638 consequences rather than directional adaptation, underscoring how dietary stress can interfere
639 with host–microbiome relationships in ways that persist beyond the period of exposure.
640 Although flies were maintained for multiple generations on a standardized diet after the
641 selection phase, microbiome differences among lines remained evident, suggesting that
642 evolutionary history of selection constrained microbial assembly long after the environmental
643 stress was removed.
644

645 Patterns in dominant bacterial phyla

646 Patterns in dominant bacterial phyla further underscore the link between microbiome dynamics
647 and host physiology. The ratio of Bacteroidota to Firmicutes decreased with age in all lines,
648 probably suggesting an age-related shift in immune potential. Previous work associates higher
649 Bacteroidota with immune activation [50] and lower Firmicutes with gut homeostasis [58]. The
650 control flies, which had higher early Proteobacteria and lower Firmicutes, may have benefited
651 from this composition. Conversely, historically stressed lines with elevated Firmicutes may carry
652 immune and metabolic imbalances linked to prior selection, leading to greater community
653 reorganization. We also observed an inverse relationship between Proteobacteria and
654 Bacteroidota in selected lines, a pattern often linked to inflammation and metabolic stress [65,
655 66]. This microbial imbalance is well-documented in human and mouse studies under high-fat or
656 sugar diets [67], suggesting deep evolutionary parallels in how dietary stress leaves microbial
657 legacies across taxa.

658

659 Microbiome succession and indicator taxa

660 Indicator species analysis showed rapid microbiome restructuring early in adulthood. Most
661 microbial turnover occurred at T1, reinforcing the importance of early life as a window for
662 microbiome establishment. While many groups declined over time, only a few were enriched in
663 specific treatments, suggesting that historical exposure to dietary stress shaped which taxa
664 persisted, rather than implying active adaptation of the microbial community. The presence of
665 potentially pro-inflammatory species such as *Porphyromonas bennonis* and *Cutibacterium*
666 *acnes* in some selection treatments raises further concern. These taxa are linked with chronic
667 inflammation in mammals [68], and their persistence in flies may indicate long-term
668 consequences for immune homeostasis. The apparent protective role of *Lactobacillus* in some
669 groups aligns with studies highlighting its antagonistic effect on pathogens [69]. Thus, persistent
670 survival differences among selection lines may result from retained microbial assemblages

capable of modulating immune and metabolic balance, rather than ongoing adaptive co-evolution.

## Limitations and future directions

Our experimental design imposed a shared long-term post-selection environment, which could mask environment-specific adaptive responses. Moreover, fewer flies from the CH and FA groups survived to late age points, limiting effective comparisons at T3. Another limitation is that we did not characterize the initial microbiome prior to experimental evolution or immediately after the selection phase, which would have helped determine the magnitude of microbiome evolution in both the control and selected lines before rearing on NutriFly. Additionally, this experiment was not originally designed with microbiome evolution as a focal endpoint; thus, the lack of sterility during culture, the possible introduction of environmental microbes, and the use of food preservatives may have contributed to uncontrolled microbial variation. Nevertheless, detectable and consistent patterns across selection regimes and time points long after cessation of selection strengthen the inference that historical diet and subsequent inbreeding have left persistent legacies on both survival and microbiome structure.

Future work should disentangle host and microbial contributions to longevity by directly manipulating microbial communities in selection lines, ideally using gnotobiotic models. Reciprocal microbiome transplants between lines could further test whether microbial legacies from past selection can transfer phenotypes to naïve hosts. It would also be informative to re-examine the lines on their original selection diets and to assess whether the microbiota themselves evolved genetically or simply underwent species sorting. Finally, metagenomic

694 profiling would clarify whether observed shifts reflect changes in microbial function or taxonomic
695 identity.

696 **Conclusion**

697 This study demonstrates that historical dietary selection and inbreeding leave persistent effects
698 on the host-associated microbiome, which we consider the most robust outcome of this
699 experiment. Selection lines exhibited microbial restructuring, and potential microbiome
700 imbalance, while changes in survival and sex-specific life history strategies provide
701 complementary context for interpreting these microbial patterns. These findings reinforce the
702 idea that dietary history can imprint lasting host–microbiome legacies, influencing lifespan and
703 physiological trajectories through both host genetic and microbial pathways. Given the rising
704 relevance of diet-induced metabolic disorders in humans and pets, and changing climatic
705 conditions for natural species, understanding how nutrition shapes microbial dynamics offers a
706 promising path for translational insights.
707

708 **List of abbreviations**

709 C – control group, CH – constant high availability, DA – deteriorating availability, FA –
710 fluctuating availability, DSPR – Drosophila Synthetic Population Resource, SIL – selection
711 inbred line, ΔAIC – delta Akaike Index, ASV – amplicon sequence variant, ISA – indicator
712 species analysis.
713

714 **Data availability**

715 All 16S Illumina raw reeds are available in the NCBI Sequence Reads Archive (SRA) BioProject
716 ID PRJNA1233815. Computer code to reproduce all analyses is available as a GitHub
717 repository at https://github.com/nochet/selPhenotyping/ and analysis steps laid out in a
718 ProjSteps.md file.
719

720 **Declarations**

721

722 **Ethics approval and consent to participate**

723 Not applicable. Clinical trial number: not applicable.

724

725 **Consent for publication**

726 All authors give the publisher the right to publish this work.

727

728 **Competing interests**

729 The authors declare no competing interests.

730

731 **Acknowledgments**

732 Authors thank Dr. Elizabeth G. King for discussions and Arthur K. Miller for technical assistance

733 with experimental set up.

734

735 **Funding**

736 The study was supported by a University of Missouri start-up award and a University of

737 Washington Nathan Shock Center Pilot Project award to EN. Funding bodies were not involved

738 in the design, collection of data, analysis, interpretation, and writing of the manuscript.

739

740 **Authors' contributions**

741 PKW performed 16S sequencing and analysis and wrote the manuscript. GM performed all fly

742 experiments. GSK helped with data analysis and performed critical revision of the manuscript.

743 EN conceived the study, designed experiments, analyzed data, and wrote the manuscript.

744

745

## References


1. Ley RE, Hamady M, Lozupone C, Turnbaugh PJ, Ramey RR, Bircher JS, et al. Evolution of mammals and their gut microbes. Science. 2008;320:1647–51. https://doi.org/10.1126/science.1155725.

2. Muegge BD, Kuczynski J, Knights D, Clemente JC, González A, Fontana L, et al. Diet drives convergence in gut microbiome functions across mammalian phylogeny and within humans. Science. 2011;332:970–4. https://doi.org/10.1126/science.1198719.

3. Gould AL, Zhang V, Lamberti L, Jones EW, Obadia B, Korasidis N, et al. Microbiome interactions shape host fitness. Proceedings of the National Academy of Sciences. 2018;115:E11951–60. https://doi.org/10.1073/pnas.1809349115.

4. Rudman SM, Greenblum S, Hughes RC, Rajpurohit S, Kiratli O, Lowder DB, et al. Microbiome composition shapes rapid genomic adaptation of Drosophila melanogaster. Proceedings of the National Academy of Sciences. 2019;116:20025–32. https://doi.org/10.1073/pnas.1907787116.

5. Petersen C, Hamerich IK, Adair KL, Griem-Krey H, Torres Oliva M, Hoeppner MP, et al. Host and microbiome jointly contribute to environmental adaptation. ISME J. 2023;17:1953–65. https://doi.org/10.1038/s41396-023-01507-9.

6. Härer A, Thompson KA, Schluter D, Rennison DJ. Associations between gut microbiota diversity and a host fitness proxy in a naturalistic experiment using threespine stickleback fish. Molecular Ecology. 2024;33:e17571. https://doi.org/10.1111/mec.17571.

7. Storelli G, Defaye A, Erkosar B, Hols P, Royet J, Leulier F. Lactobacillus plantarum promotes Drosophila systemic growth by modulating hormonal signals through TOR-dependent nutrient sensing. Cell Metab. 2011;14:403–14. https://doi.org/10.1016/j.cmet.2011.07.012.

8. de Weerth C. Do bacteria shape our development? Crosstalk between intestinal microbiota and HPA axis. Neuroscience & Biobehavioral Reviews. 2017;83:458–71. https://doi.org/10.1016/j.neubiorev.2017.09.016.

9. Rowe M, Veerus L, Trosvik P, Buckling A, Pizzari T. The reproductive microbiome: an emerging driver of sexual selection, sexual conflict, mating systems, and reproductive isolation. Trends in Ecology & Evolution. 2020;35:220–34. https://doi.org/10.1016/j.tree.2019.11.004.

10. Suyama R, Cetraro N, Yew JY, Kai T. Microbes control Drosophila germline stem cell increase and egg maturation through hormonal pathways. Commun Biol. 2023;6:1–18. https://doi.org/10.1038/s42003-023-05660-x.

11. Erkosar B, Storelli G, Defaye A, Leulier F. Host-intestinal microbiota mutualism: “learning on the fly.” Cell Host Microbe. 2013;13:8–14. https://doi.org/10.1016/j.chom.2012.12.004.

12. Spragge F, Bakkeren E, Jahn MT, B. N. Araujo E, Pearson CF, Wang X, et al. Microbiome diversity protects against pathogens by nutrient blocking. Science. 2023;382:eadj3502. https://doi.org/10.1126/science.adj3502.

783 13. Christensen SM, Srinivas SN, McFrederick QS, Danforth BN, Buchmann SL, Vannette RL.
784 Symbiotic bacteria and fungi proliferate in diapause and may enhance overwintering survival in
785 a solitary bee. The ISME Journal. 2024;18:wrae089. https://doi.org/10.1093/ismejo/wrae089.

786 14. Clark RI, Salazar A, Yamada R, Fitz-Gibbon S, Morselli M, Alcaraz J, et al. Distinct shifts in
787 microbiota composition during Drosophila aging impair intestinal function and drive mortality.
788 Cell Reports. 2015;12:1656–67. https://doi.org/10.1016/j.celrep.2015.08.004.

789 15. Aleman FDD, Valenzano DR. Microbiome evolution during host aging. PLOS Pathogens.
790 2019;15:e1007727. https://doi.org/10.1371/journal.ppat.1007727.

791 16. Broderick NA, Buchon N, Lemaitre B. Microbiota-induced changes in Drosophila
792 melanogaster host gene expression and gut morphology. mBio. 2014;5:10.1128/mbio.01117-14.
793 https://doi.org/10.1128/mbio.01117-14.

794 17. Shapira M. Gut microbiotas and host evolution: scaling up symbiosis. Trends in Ecology &
795 Evolution. 2016;31:539–49. https://doi.org/10.1016/j.tree.2016.03.006.

796 18. Okin D, Medzhitov R. Evolution of inflammatory diseases. Current Biology. 2012;22:R733–
797 40. https://doi.org/10.1016/j.cub.2012.07.029.

798 19. Wong A, Chaston J, Douglas A. The inconstant gut microbiota of Drosophila species
799 revealed by 16S rRNA gene analysis. The ISME journal. 2013;7.
800 https://doi.org/10.1038/ismej.2013.86.

801 20. Martino ME, Joncour P, Leenay R, Gervais H, Shah M, Hughes S, et al. Bacterial adaptation
802 to the host's diet is a key evolutionary force shaping Drosophila-Lactobacillus symbiosis. Cell
803 Host Microbe. 2018;24:109-119.e6. https://doi.org/10.1016/j.chom.2018.06.001.

804 21. Wong AC-N, Dobson AJ, Douglas AE. Gut microbiota dictates the metabolic response of
805 Drosophila to diet. Journal of Experimental Biology. 2014;217:1894–901.
806 https://doi.org/10.1242/jeb.101725.

807 22. Lee KP, Simpson SJ, Clissold FJ, Brooks R, Ballard JWO, Taylor PW, et al. Lifespan and
808 reproduction in Drosophila: new insights from nutritional geometry. Proc Natl Acad Sci U S A.
809 2008;105:2498–503. https://doi.org/10.1073/pnas.0710787105.

810 23. Simpson SJ, Raubenheimer D. Macronutrient balance and lifespan. Aging (Albany NY).
811 2009;1:875–80. https://doi.org/10.18632/aging.100098.

812 24. Piper MDW, Partridge L, Raubenheimer D, Simpson SJ. Dietary restriction and aging: a
813 unifying perspective. Cell Metab. 2011;14:154–60. https://doi.org/10.1016/j.cmet.2011.06.013.

814 25. Skorupa DA, Dervisefendic A, Zwiener J, Pletcher SD. Dietary composition specifies
815 consumption, obesity, and lifespan in Drosophila melanogaster. Aging Cell. 2008;7:478–90.
816 https://doi.org/10.1111/j.1474-9726.2008.00400.x.

817 26. Grandison RC, Piper MDW, Partridge L. Amino-acid imbalance explains extension of
818 lifespan by dietary restriction in Drosophila. Nature. 2009;462:1061–4.
819 https://doi.org/10.1038/nature08619.

820 27. Sannino DR, Dobson AJ, Edwards K, Angert ER, Buchon N. The Drosophila melanogaster
821 gut microbiota provisions thiamine to its host. mBio. 2018;9:10.1128/mbio.00155-18.
822 https://doi.org/10.1128/mbio.00155-18.

823 28. Arias-Rojas A, Iatsenko I. The role of microbiota in Drosophila melanogaster aging.
824 Frontiers in Aging. 2022;3.

825 29. King EG, Macdonald SJ, Long AD. Properties and power of the Drosophila Synthetic
826 Population Resource for the routine dissection of complex traits. Genetics. 2012;191:935–49.
827 https://doi.org/10.1534/genetics.112.138537.

828 30. King EG, Merkes CM, McNeil CL, Hoofer SR, Sen S, Broman KW, et al. Genetic dissection
829 of a model complex trait using the Drosophila Synthetic Population Resource. Genome Res.
830 2012;22:1558–66. https://doi.org/10.1101/gr.134031.111.

831 31. Ng'oma E, Fidelis W, Middleton KM, King EG. The evolutionary potential of diet-dependent
832 effects on lifespan and fecundity in a multi-parental population of Drosophila melanogaster.
833 Heredity. 2019;122:582–94. https://doi.org/10.1038/s41437-018-0154-2.

834 32. Pool JE. The mosaic ancestry of the Drosophila Genetic Reference Panel and the D.
835 melanogaster Reference Genome reveals a network of epistatic fitness interactions. Molecular
836 Biology and Evolution. 2015;32:3236–51. https://doi.org/10.1093/molbev/msv194.

837 33. Bass TM, Grandison RC, Wong R, Martinez P, Partridge L, Piper MDW. Optimization of
838 dietary restriction protocols in Drosophila. J Gerontol A Biol Sci Med Sci. 2007;62:1071–81.
839 https://doi.org/10.1093/gerona/62.10.1071.

840 34. Chapman T, Liddle LF, Kalb JM, Wolfner MF, Partridge L. Cost of mating in Drosophila
841 melanogaster females is mediated by male accessory gland products. Nature. 1995;373:241–4.
842 https://doi.org/10.1038/373241a0.

843 35. Wigby S, Chapman T. Sex peptide causes mating costs in female Drosophila melanogaster.
844 Curr Biol. 2005;15:316–21. https://doi.org/10.1016/j.cub.2005.01.051.

845 36. Jones A, Donnell D, King EG, Ng'oma E. Larval protein restriction interacts with adult diet to
846 increase fitness in an outbred multiparent population. 2024;:2024.02.10.579751.
847 https://doi.org/10.1101/2024.02.10.579751.

848 37. Walters WA, Caporaso JG, Lauber CL, Berg-Lyons D, Fierer N, Knight R. PrimerProspector:
849 de novo design and taxonomic analysis of barcoded polymerase chain reaction primers.
850 Bioinformatics. 2011;27:1159–61. https://doi.org/10.1093/bioinformatics/btr087.

851 38. Caporaso JG, Lauber CL, Walters WA, Berg-Lyons D, Lozupone CA, Turnbaugh PJ, et al.
852 Global patterns of 16S rRNA diversity at a depth of millions of sequences per sample.
853 Proceedings of the National Academy of Sciences. 2011;108 supplement_1:4516–22.
854 https://doi.org/10.1073/pnas.1000080107.

855 39. Callahan BJ, McMurdie PJ, Rosen MJ, Han AW, Johnson AJA, Holmes SP. DADA2: High-
856 resolution sample inference from Illumina amplicon data. Nat Methods. 2016;13:581–3.
857 https://doi.org/10.1038/nmeth.3869.

858 40. Simhadri RK, Fast EM, Guo R, Schultz MJ, Vaisman N, Ortiz L, et al. The gut commensal
859 microbiome of Drosophila melanogaster is modified by the endosymbiont wolbachia. mSphere.
860 2017;2:e00287-17. https://doi.org/10.1128/mSphere.00287-17.

861 41. McMurdie PJ, Holmes S. phyloseq: an R package for reproducible interactive analysis and
862 graphics of microbiome census data. PLOS ONE. 2013;8:e61217.
863 https://doi.org/10.1371/journal.pone.0061217.

864 42. Greenacre M, Martínez-Álvaro M, Blasco A. Compositional data analysis of microbiome and
865 any-omics datasets: a validation of the additive logratio transformation. Front Microbiol.
866 2021;12. https://doi.org/10.3389/fmicb.2021.727398.

867 43. Karwowska Z, Aasmets O, Metspalu M, Metspalu A, Milani L, Esko T, et al. Effects of data
868 transformation and model selection on feature importance in microbiome classification data.
869 Microbiome. 2025;13:2. https://doi.org/10.1186/s40168-024-01996-6.

870 44. McKnight DT, Huerlimann R, Bower DS, Schwarzkopf L, Alford RA, Zenger KR. Methods for
871 normalizing microbiome data: An ecological perspective. Methods in Ecology and Evolution.
872 2019;10:389–400. https://doi.org/10.1111/2041-210X.13115.

873 45. Paradis E, Claude J, Strimmer K. APE: analyses of phylogenetics and evolution in R
874 language. Bioinformatics. 2004;20:289–90. https://doi.org/10.1093/bioinformatics/btg412.

875 46. Oksanen J, Blanchet FG, Kindt R, Legendre P, Minchin P, O'Hara R, et al. Vegan:
876 community ecology package. R package vegan, vers. 2.2-1. 2015.

877 47. Anderson MJ. Distance-based tests for homogeneity of multivariate dispersions. Biometrics.
878 2006;62:245–53. https://doi.org/10.1111/j.1541-0420.2005.00440.x.

879 48. Cáceres MD, Legendre P. Associations between species and groups of sites: indices and
880 statistical inference. Ecology. 2009;90:3566–74. https://doi.org/10.1890/08-1823.1.

881 49. Sultanova Z, Dönertaş HM, Hita A, Aguilar P, Dag B, Lucas-Lledo JI, et al. Age-dependent
882 gut microbiota dynamics and their association with male fitness traits in Drosophila
883 melanogaster. 2025;:2025.05.22.655607. https://doi.org/10.1101/2025.05.22.655607.

884 50. Shen X, Miao J, Wan Q, Wang S, Li M, Pu F, et al. Possible correlation between gut
885 microbiota and immunity among healthy middle-aged and elderly people in southwest China.
886 Gut Pathogens. 2018;10:4. https://doi.org/10.1186/s13099-018-0231-3.

887 51. Gibbons J, Yoo JY, Mutka T, Groer M, Ho TTB. A pilot study to establish an in vitro model to
888 study premature intestinal epithelium and gut microbiota interactions. mSphere.
889 2021;6:10.1128/msphere.00806-21. https://doi.org/10.1128/msphere.00806-21.

890 52. Stanley PD, Ng'oma E, O'Day S, King EG. Genetic dissection of nutrition-induced plasticity
891 in insulin/insulin-like growth factor signaling and median life span in a *Drosophila* multiparent
892 population. Genetics. 2017;206:587–602. https://doi.org/10.1534/genetics.116.197780.

893 53. Ng'oma E, Williams-Simon PA, Rahman A, King EG. Diverse biological processes
894 coordinate the transcriptional response to nutritional changes in a Drosophila melanogaster

895 multiparent population. BMC Genomics. 2020;21:84. https://doi.org/10.1186/s12864-020-6467-
896 6.

897 54. Rose MR, Charlesworth B. Genetics of life history in Drosophila melanogaster. I. sib
898 analysis of adult females. Genetics. 1981;97:173–86.

899 55. Kawecki TJ, Ebert D. Conceptual issues in local adaptation. Ecology Letters. 2004;7:1225–
900 41. https://doi.org/10.1111/j.1461-0248.2004.00684.x.

901 56. Leitão-Gonçalves R, Carvalho-Santos Z, Francisco AP, Fioreze GT, Anjos M, Baltazar C, et
902 al. Commensal bacteria and essential amino acids control food choice behavior and
903 reproduction. PLOS Biology. 2017;15:e2000862. https://doi.org/10.1371/journal.pbio.2000862.

904 57. Staubach F, Baines JF, Künzel S, Bik EM, Petrov DA. Host species and environmental
905 effects on bacterial communities associated with Drosophila in the laboratory and in the natural
906 environment. PLOS ONE. 2013;8:e70749. https://doi.org/10.1371/journal.pone.0070749.

907 58. Lee H-Y, Lee S-H, Lee J-H, Lee W-J, Min K-J. The role of commensal microbes in the
908 lifespan of Drosophila melanogaster. Aging (Albany NY). 2019;11:4611–40.
909 https://doi.org/10.18632/aging.102073.

910 59. Blum JE, Fischer CN, Miles J, Handelsman J. Frequent replenishment sustains the
911 beneficial microbiome of Drosophila melanogaster. mBio. 2013;4:10.1128/mbio.00860-13.
912 https://doi.org/10.1128/mbio.00860-13.

913 60. Chandler JA, Lang JM, Bhatnagar S, Eisen JA, Kopp A. Bacterial communities of diverse
914 Drosophila species: Ecological context of a host–microbe model system. PLOS Genetics.
915 2011;7:e1002272. https://doi.org/10.1371/journal.pgen.1002272.

916 61. Brummel T, Ching A, Seroude L, Simon AF, Benzer S. Drosophila lifespan enhancement by
917 exogenous bacteria. Proceedings of the National Academy of Sciences. 2004;101:12974–9.
918 https://doi.org/10.1073/pnas.0405207101.

919 62. Shin SC, Kim S-H, You H, Kim B, Kim AC, Lee K-A, et al. Drosophila microbiome modulates
920 host developmental and metabolic homeostasis via insulin signaling. Science. 2011;334:670–4.
921 https://doi.org/10.1126/science.1212782.

922 63. Newell PD, Douglas AE. Interspecies interactions determine the impact of the gut microbiota
923 on nutrient allocation in Drosophila melanogaster. Appl Environ Microbiol. 2014;80:788–96.
924 https://doi.org/10.1128/AEM.02742-13.

925 64. Obata F, Fons CO, Gould AP. Early-life exposure to low-dose oxidants can increase
926 longevity via microbiome remodelling in Drosophila. Nat Commun. 2018;9:975.
927 https://doi.org/10.1038/s41467-018-03070-w.

928 65. Mukhopadhya I, Hansen R, El-Omar EM, Hold GL. IBD-what role do Proteobacteria play?
929 Nat Rev Gastroenterol Hepatol. 2012;9:219–30. https://doi.org/10.1038/nrgastro.2012.14.

930 66. Shin N-R, Whon TW, Bae J-W. Proteobacteria: microbial signature of dysbiosis in gut
931 microbiota. Trends Biotechnol. 2015;33:496–503. https://doi.org/10.1016/j.tibtech.2015.06.011.

932 67. Bradley PH, Pollard KS. Proteobacteria explain significant functional variability in the human
933 gut microbiome. Microbiome. 2017;5:36. https://doi.org/10.1186/s40168-017-0244-z.

934 68. Caselli E, Soffritti I, D'Accolti M, Piva I, Greco P, Bonaccorsi G. Atopobium vaginae and
935 Porphyromonas somerae induce proinflammatory cytokines expression in endometrial cells: a
936 possible implication for endometrial cancer? Cancer Manag Res. 2019;11:8571–5.
937 https://doi.org/10.2147/CMAR.S217362.

938 69. Moses RP, Y. Dawood H, Fashemi T, N. Fichorova R, Onderdonk AB, S. Yamamoto H.
939 Lactobacillus curbs inflammatory responses to atopobium vaginae. Obstetrics & Gynecology.
940 2015;125:3S. https://doi.org/10.1097/01.AOG.0000463525.50901.93.

941